Influence of oxygen partial pressure on the oxygen diffusion and surface exchange coefficients in mixed conductors

Pierre-Marie Geffroy, Laure Guironnet, Henry J. M. Bouwmeester, Thierry Chartier, Jean-Claude Grenier, Jean-Marc. Bassat

Influence of oxygen partial pressure on the oxygen diffusion and surface exchange coefficients in mixed conductors

P.-M. GEFFROY[1], L. GUIRONNET[1,2], H.J.M. BOUWMEESTER[3], T. CHARTIER[1], J.-C. GRENIER[4], and J.-M. BASSAT[4]

[1] SPCTS, CNRS, ENSCI, Université de Limoges, CEC, 12 Rue Atlantis 87068 LIMOGES, France
[2] ADEME, 20 avenue du Grésillé, BP 90406, 49004 ANGERS cedex 1, France
[3] University of Twente, Enschede, Neteherlands
[4] ICMCB - CNRS, 87 Avenue du docteur Schweitzer, 33608 PESSAC, France

Corresponding author Email: pierre-marie.geffroy@unilim.fr

Keywords: *Mixed conductor, Oxygen surface exchanges, Oxygen isotopic exchange, Oxygen partial pressure*

Abstract

The performances of mixed ionic and electronic conductors is used in many applications, such as oxygen transport membranes or electrodes in solid oxide fuel cells. The performances of these systems depend mainly on two fundamental parameters including oxygen diffusion (D_O) and the oxygen exchange coefficient (k). This work focuses on the impact of the oxygen partial pressure on oxygen diffusion and surface exchange coefficients of mixed conducting materials, as reported studies are scarce in the literature. In this way, two different mixed conducting materials are studied, namely, $La_{0.6}Sr_{0.4}Fe_{0.6}Ga_{0.4}O_{3-\delta}$, a perovskite-type material, and the nickelate $La_2NiO_{4+\delta}$. The D_O and k coefficients are determined by a specific oxygen permeation measurement and by the isotopic exchange depth profile method.

1. Introduction

Mixed ionic and electronic conducting materials (MIEC) are of great interest with respect to the development of Catalytic Membrane Reactors (CMR) as well as oxygen separation (semi-permeation) devices. High electronic and ionic conductivities, as well as good kinetics of oxygen surface exchanges, are required. Oxygen diffusion (related to the oxide ionic conductivity) and/or oxygen surface exchange, characterized by the D_O and k coefficients could be the limiting parameters with respect to the electrochemical performances of the systems.

D_O and k can be determined by 1) designing a specific setup to measure at the same oxygen semi-permeation flux and the activity gradient at both membrane surfaces and 2) using the so-called IEDP (Isotopic Exchange Depth Profile) method coupled with SIMS performed on dense pellets. The oxygen partial pressure at the surface of the studied material can be highly different on both faces of the pellet, especially in the case of semi-permeation devices, where the pO_2 ratio between the oxygen-rich and oxygen-lean environments is approximately 10^4-10^5. As a consequence, it is of high importance to include pO_2 as an additional experimental parameter to clearly identify the rate determining steps. The data reported in the literature regarding the pO_2 dependence of D_O or k are scarce. However, most electrochemical systems at high temperature operate under a large range of pO_2, solid oxide fuels, cells, gas sensors, and oxygen transport membranes.

In this work, two different MIEC materials are studied. i) The first material is an oxygen deficient perovskite, $La_{0.6}Sr_{0.4}Fe_{0.6}Ga_{0.4}O_{3-\delta}$ (hereafter called LSFG6464), and ii) the second material, $La_2NiO_{4+\delta}$ (hereafter called LNO), is a Ruddlesden-Popper (n=1)-type compound showing additional oxygen species. These two materials show also two different crystal structures and mechanisms of oxygen diffusion in order to generalize the results of this paper to other materials.

The D_O and k coefficients are independently determined as a function of temperature and oxygen partial pressure and compared to data reported in the literature. The values obtained by two methods are compared and also discussed in this work.

2. Experiments

2.1 Staring materials

LSFG6464 and LNO powders were synthesized using the solid-state reaction and the nitrate-citrate route, respectively. The oxygen semi-permeation measurements were performed using dense disk samples with a thickness of 1 mm and a diameter of 23-24 mm, while the oxygen isotopic exchange measurements were performed using dense disk samples with a thickness of 2 mm and a diameter of 6 mm obtained by a tape casting process. Both materials had a relative density higher than 99% after sintering.

2.2 Isotopic Exchange Depth Profile method

The oxygen diffusion coefficient was measured using the Isotope Exchange Depth Profile (IEDP) technique, *i.e.,* determining the penetration depth profiles of the oxygen isotope ^{18}O used as a tracer [2]. The isotope exchanges between ^{18}O gas and the pellet were performed at 800°C, and the chamber volume is approximately 100 cm^3. The measured penetration profile can be fitted using a solution for Fick's second law, from which the D* and k* coefficients (*refers to the tracer) can be extracted [2].

An example of the evolution of the ^{18}O profiles through a $La_{0.6}Sr_{0.4}Fe_{0.6}Ga_{0.4}O_{3-\delta}$ (LSFG6464) pellet at 800°C for two different pO_2 values is given in Figure 1. The profile is deeper when pO_2 increases.

2.3 Oxygen semi-permeation method

The oxygen semi-permeation measurements were performed using a homemade device described in a previous work [1]. It is built with a central reactor where the dense membrane is inserted between two chambers with two different oxygen partial pressures. In each chamber, two microelectrodes (gold and zirconia tip electrodes) in contact with the surface of the membrane allow the oxygen potential gradients between the surface and the gas at the vicinity of the surface to be determined (annex 2).

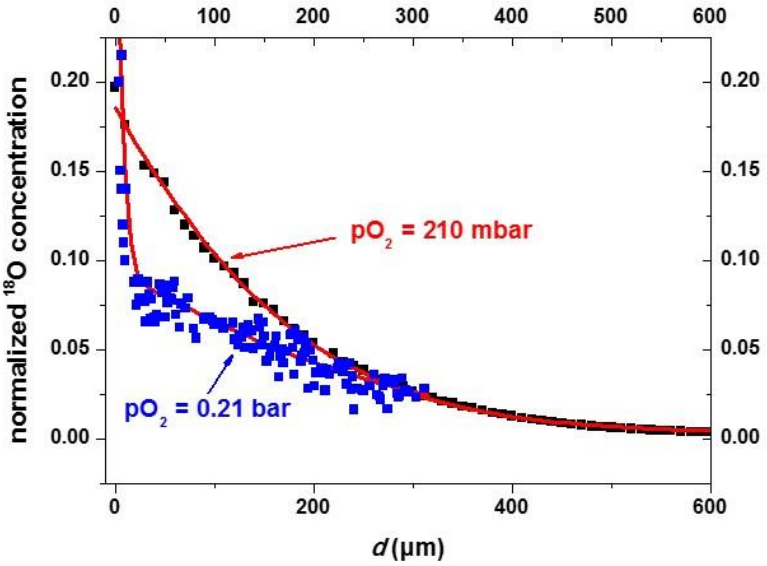

Figure 1: Normalized ^{18}O concentration profiles recorded through an LSFG6464 pellet at 800°C for 3600 s under p = 210 mbar (line-scanning method, black dots) and under p = 21 mbar (imaging mode, blue dots). The corresponding fits are added (red lines).

3. Results and Discussion

3.1 Determination of D and k by isotopic exchanges

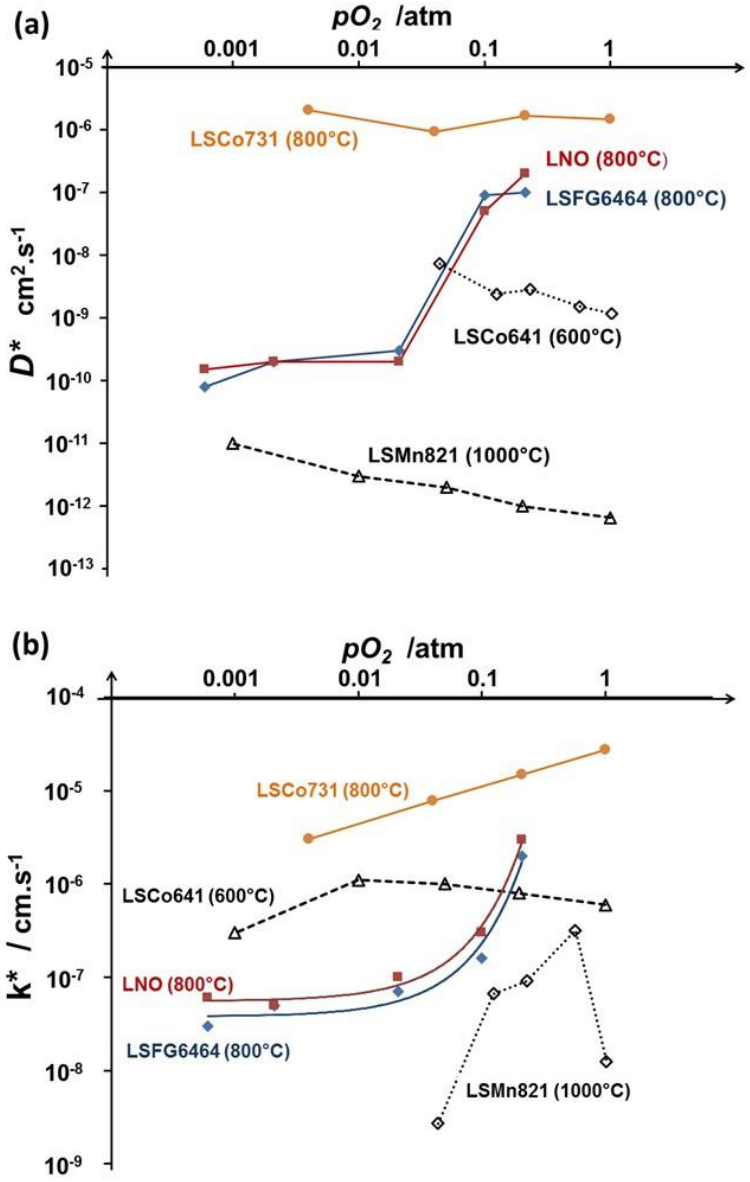

Figure 2: pO_2 dependence on a) D* and b) k* of the following mixed conductors: $La_{0.6}Sr_{0.4}Fe_{0.6}Ga_{0.4}O_{3-\delta}$ (LSFG6464) at 800°C, $La_2NiO_{4+\delta}$ (LNO) at 800°C, $La_{0.7}Sr_{0.3}CoO_{3-\delta}$ (LSCo731) at 800°C [3], $La_{0.8}Sr_{0.2}MnO_{3-\delta}$ (LSMn821) at 1000°C [4] and $La_{0.6}Sr_{0.4}CoO_{3-\delta}$ (LSCo641) at 600°C [5].

Figure 2 shows the data collected in the literature regarding the pO_2 dependence on D* and k* for exclusively mixed conducting materials. The D* and k* coefficients show very different evolution with pO_2 for each material. For instance, D* at 800°C for $La_{0.7}Sr_{0.3}CoO_{3-\delta}$ (LSCo731) is stable with pO_2 while D* at 1000°C for $La_{0.8}Sr_{0.2}MnO_{3-\delta}$ (LSMn821) increases when the pO_2 decreases. It is not possible to confirm the general trend of the pO_2 dependence on D* and k* from the data collected in the literature. However, for most mixed conductors, the k* coefficient decreases significantly with pO_2 (one or two orders of magnitude from 0.21 to 0.001 atm.), and the D* coefficient shows low variation for high pO_2.

In this work, values of D* and k* decrease significantly with pO_2, particularly below 0.1 atm. Indeed, the IEDP method requires no variation of ^{18}O concentration in the chamber during the isotope exchanges at high temperature. This assumption is true if the quantity of ^{18}O orpO_2 is large with a large chamber volume. Then, when pO_2 is lower than 0.1 atm., the concentration of ^{18}O in the chamber decreases significantly during the isotope exchanges due to the ^{18}O penetration in the sample. The decrease of ^{18}O concentration in gas also involves a low penetration of ^{18}O in the sample or an underestimation of D* and k* values. As shown in table 1, it is assumed that the quantity of ^{18}O decreases quickly in the chamber during the exchange period, as the ratio between ^{18}O moles in the gas and oxygen moles in the pellet sample decreases. In optimal conditions, this ratio must be close to or higher than unity; then, these conditions are true only when $pO_2 \geq 0.1$.

pO_2 in ^{18}O (atm.)	Quantity of ^{18}O in gas (mol) (chamber volume=100 cm^3)	Estimated quantity of ^{18}O in the pellet (mol) after exchange	Ratio ^{18}O mol (gas) / ^{18}O mol in the pellet
0.21	$2.3\ 10^{-4}$	$1.3\ 10^{-4}$	1.8
0.1	$1.1\ 10^{-4}$	$5\ 10^{-5}$	2.3
0.02	$2.2\ 10^{-5}$	$5\ 10^{-4}$	0.05
0.002	$2.2\ 10^{-6}$	$3\ 10^{-4}$	0.007
0.0005	$5.6\ 10^{-7}$	$2.5\ 10^{-4}$	0.002

Table 1: Evolution of ^{18}O quantity in the gas in relation to pO_2.

3.2 Determination of D_O and k by semi-permeation measurements

In the oxygen semi-permeation phenomenon, the diffusion step by volume is usually considered to be the limiting step in oxygen transport through a membrane, as described in Wagner's law. However, the measurements obtained with the electrode system in recent works show that the chemical potential of oxygen at the surface of the membrane is not in balance with that of the gas at the surface vicinity [1, 6], as reported in Figure 2.

Thus, Wagner's law must account for the oxygen chemical potential gradient at the membrane surfaces $(\Delta\mu_{O2}^{surf})$, as described in Figure 3. Then, a linear relationship can be established between the oxygen flux and the driving forces (or oxygen chemical potential gradient) in bulk and without the contribution of oxygen surface exchange, as expected by the use of Wagner's law [7].

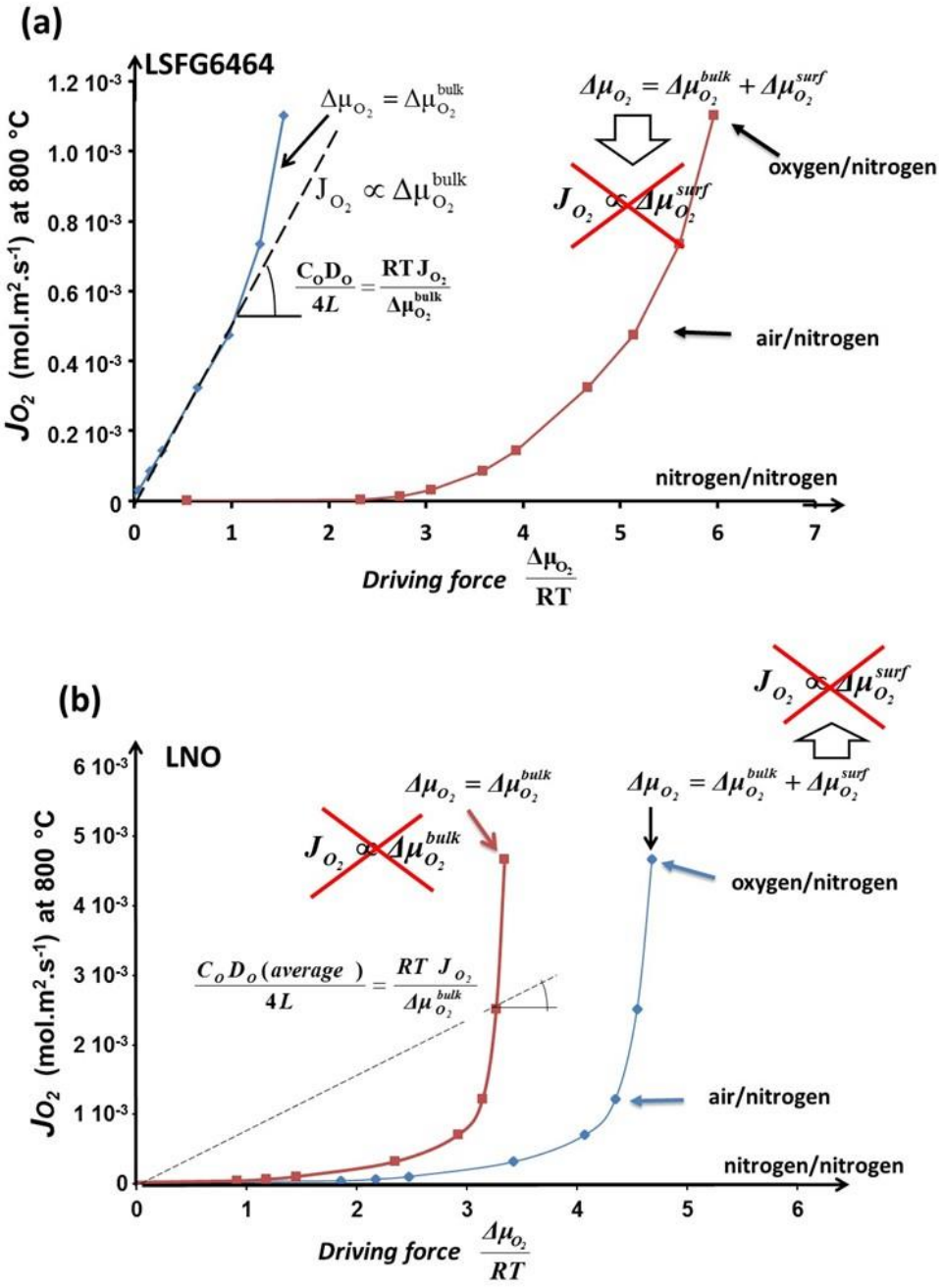

Figure 3: Relationship between the oxygen flux obtained with a) an LSFG6464 perovskite membrane and b) an LNO membrane at 800°C and driving forces with and without the contribution of surface exchanges.

3.2.1 Determination of D_O

The LSFG6464 and LNO materials are the predominant electronic conductors [4, 6] because the mobility of electronic carriers is generally larger than that of ionic carriers, i.e., $\sigma_e >> \sigma_{ion}$. Then, Wagner's law can be expressed as equation 1 as follows:

$$J_{O_2} = \frac{\sigma_{ion}}{16FL} \Delta\mu_{O_2}^{Bulk} \qquad \text{equation 1}$$

J_{O_2} is the oxygen flux through the membrane

L is the thickness of the membrane,
R is the universal gas constant,
F is Faraday's constant,

σ_{ion} is ionic conductivity.

$\Delta\mu_{O_2}^{Bulk}$ corresponds to gradient of oxygen chemical potential through the bulk of membrane

The Nernst-Einstein relationship (equation 2) can express the ionic conductivity under a pO_2 gradient based on the average values of both the chemical diffusion coefficient of oxygen (D_O) through the membrane and the molar concentration of oxygen (C_O) as follows:

$$\sigma_{ion} = \frac{4F^2 C_O D_O}{RT} \qquad \text{equation 2}$$

C_O: average molar concentration of oxygen in the bulk of the membrane.

From the Nernst-Einstein relationship and equation 2, the oxygen flux and oxygen diffusion coefficient are described as follows:

and

$$D_O = \frac{4RTL}{C_O \Delta\mu_{O_2}^{Bulk}} J_{O_2} \qquad \text{equation 3}$$

The chemical diffusion coefficient of oxygen (D_O) is considered constant over the thickness of the membrane in the steady state and assuming a random distribution of oxygen vacancies in the crystal lattice. In other terms, the chemical diffusion coefficient of the oxygen measured by semi-permeation corresponds to the average diffusion coefficient in the range from pO_2 in gas on oxygen rich and lean sides of the membrane.

Furthermore, the oxygen tracer diffusion coefficient D_O^* is proportional to D_O by a Haven factor (H_v) [8] (equation 6).

$$D_O^* = H_V D_O \qquad \text{equation 6}$$

For an ideal perovskite structure, the factor H_v is equal to 0.69 [7] since, for LNO materials corresponding to an interstitial oxygen mechanism, it is assumed that H_v is close to unity [8].

3.2.2 Determination of k

Usually, both cases are considered in the expression of the oxygen surface exchange kinetics, for which the chemical potential gradient at the membrane surface is either large or small.

Adler *et al.* suggested a rigorous definition of the surface exchange laws in the case of a mixed conductor using a formalism related to the thermodynamics of irreversible processes and mass action laws [9]. Starting from this formalism, the following relationship can be established based on the Butler-Volmer equation. More recently, M. Bazant proposed a similar formalism for the ionic species exchanges at the solid interface electrode/electrolyte in batteries [10]. It should be noted that the proposed formalism is different from the one previously reported by Kim *et al.* [11].

$$J_O = kC_O\left(\exp\left(\frac{(1-\beta)}{RT}\Delta\mu_O^{surf}\right) - \exp\left(\frac{-\beta}{RT}\Delta\mu_O^{surf}\right)\right)$$ equation 7

J_O: Oxygen flux through the membrane surface.
C_O: Molar concentration of oxygen in the vicinity of the membrane surface.
β: Asymmetric coefficient depending on the nature of the transition state and composition. This parameter considers the asymmetric energetic barrier due to the O^{2-} anions crossing a polarized solid/gas interface with an electronic charge transfer.
$\Delta\mu_O^{surf}$: The gradient of the oxygen chemical potential between the gas and the surface of the membrane. In other works, this term usually corresponds to the driving force of oxygen flux, called affinity. In this work, this term is directly measured by two microelectrodes in contact with the membrane surface [1]. Additionally, it is worth noting that the Butler-Volmer formalism defines the driving force as $\eta = \Delta\mu_O^{surf}/mF$ with *m* and the electron transfer number in the interfacial reaction.

It follows that

$$\Delta\mu_O^{surf} = \frac{1}{2}\Delta\mu_{O_2}^{surf}$$ equation 8

$$J_O = \frac{1}{2}J_{O_2}$$ equation 9

Then, equation 7 becomes

$$J_{O_2} = \frac{1}{2}kC_O\left(\exp\left(\frac{(1-\beta)}{2RT}\Delta\mu_{O_2}^{surf}\right) - \exp\left(\frac{-\beta}{2RT}\Delta\mu_{O_2}^{surf}\right)\right)$$ equation 10

Equation 10 can be simplified by a linear relation in equation 11, if $\Delta\mu_{O_2}^{surf} < RT$, as reported in Figure 3.

$$J_{O_2} = \frac{kC_O}{4RT}\Delta\mu_{O_2}^{surf}$$ equation 11

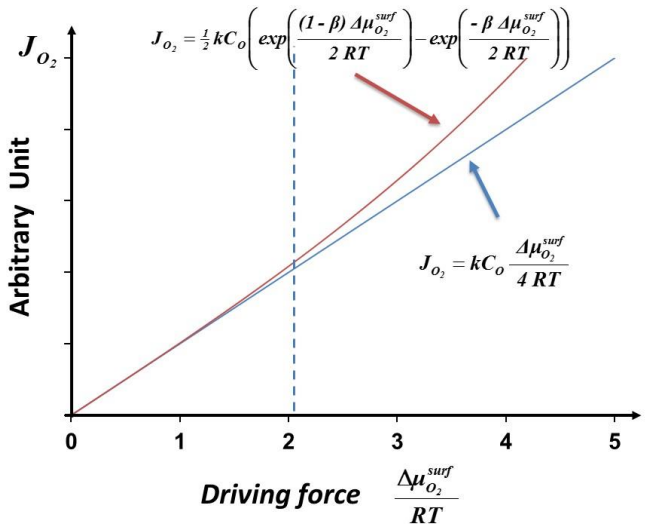

Figure 4: Comparative evolution of the oxygen flux (JO_2) with the driving force $\frac{\Delta\mu_{O2}^{surf}}{RT}$ from a linear approximate relation and a relation based on the Butler-Volmer formalism with an arbitrary value of β=0.5.

Figure 4 shows that the usual linear relation reported in the literature [12] corresponds to a good approximation within a large range of gradients. The discrepancy between both models becomes significant only if $\Delta\mu_{O_2}^{surf} > 3 \text{ or } 4$ RT. The linear relation reported in equation 11 can be applied in most cases. However, Figure 2 shows that the oxygen chemical potential gradient at the membrane surface in contact with oxygen lean atmosphere is very large, up to 3 RT for LSFG6464 membranes. This suggests that the Butler-Volmer formalism must be applied in this case, as reported in equation 10.

A large oxygen chemical potential gradient at the surface

In this case, $\Delta\mu_{O_2}^{surf(rich)}$ and $\Delta\mu_{O_2}^{surf(lean)} > 2$RT, Surface exchanges are then described by an exponential relation of the chemical potential decrease at the oxygen rich surface (equation 12) and through the oxygen lean surface (equation 13).

$$k^{rich} = \frac{2J_{O_2}}{C_O^{rich}\left(exp\left(\frac{(1-\beta)}{2RT}\Delta\mu_{O_2}^{surf(rich)}\right) - exp\left(\frac{-\beta}{2RT}\Delta\mu_{O_2}^{surf(rich)}\right)\right)} \qquad \text{equation 12}$$

$$k^{lean} = \frac{2J_{O_2}}{C_O^{lean}\left(exp\left(\frac{(1-\beta)}{2RT}\Delta\mu_{O_2}^{surf(lean)}\right) - exp\left(\frac{-\beta}{2RT}\Delta\mu_{O_2}^{surf(lean)}\right)\right)} \qquad \text{equation 13}$$

where k is the oxygen surface exchange coefficient, C_O^{rich} and C_O^{lean} are the oxygen molar concentrations in the membrane at vicinity of the oxygen rich and lean surfaces, and $\Delta\mu_{O_2}^{surf(rich)}$ and $\Delta\mu_{O_2}^{surf(lean)}$, are the gradient of oxygen chemical potentials through the membrane surface in contact with the oxygen rich and oxygen lean atmospheres, respectively (see Table 2 in the annex). The β exponent coefficient is constant and is between 0 and 1 [9,10].

Equations 14 and 15 are two expressions of the oxygen surface coefficient (k) at the oxygen partial pressure corresponding to the oxygen partial pressure close to equilibrium with the membrane surface. These pressures are measured using a system of microelectrodes at the oxygen-lean and oxygen-rich surfaces of the membrane.

From the measurement of the oxygen potential gradient at both membrane surfaces and using equations 14 and 15, we were able to determine the surface exchange coefficients at the oxygen-rich and the oxygen-lean membrane faces, k^{rich} and k^{lean}, as a function of pO_2.

A low oxygen chemical potential gradient at the surface

In the case of a low chemical potential gradient at the surface, $\Delta\mu_{O_2}^{surf(rich)}$ *and* $\Delta\mu_{O_2}^{surf(lean)} < 2RT$, equations 12 and 13 become, respectively :

$$k^{rich} = \frac{4RT\,J_{O_2}}{C_O^{rich}\,\Delta\mu_{O_2}^{surf(rich)}} \qquad \text{equation 14}$$

and

$$k^{lean} = \frac{4RT\,J_{O_2}}{C_O^{lean}\,\Delta\mu_{O_2}^{surf(lean)}} \qquad \text{equation 15}$$

Equations 14 and 15 show the usual linear relationship between the oxygen flux (J_{O_2}) and the driving force ($\Delta\mu_{O_2}^{surf}$) with the pO_2 dependence of k^{lean} and k^{rich} coefficients as reported by Bouwmeester *et al.* [12]. Then, both coefficients can be compared to the k* coefficient obtained by the IEDP method, as reported by De Souza [13].

3.3 pO_2 dependence of D_O and k

Previous work reported by De Souza et al. shows the dependence of D* and k* obtained by the isotopic exchange method as a function of pO_2 for several perovskite (oxygen deficient) materials [13]. In particular, the pO_2 dependence of k* obeys a power law, as described in equation 16.

$$k^* = k_0 \left(\frac{pO_2}{pO_2^\circ}\right)^n \qquad \text{equation 16}$$

where k_O is the surface exchange coefficient at the reference oxygen partial pressure, usually pO_2° = 0.21 atm, n is the power law parameter related to the electronic defect concentration in these materials as follows: n = 0.23 for ionic conductors ($Ce_{0.8}Gd_{0.2}O_{2-\delta}$ and $La_{0.9}Sr_{0.1}Ga_{0.8}Mg_{0.2}O_{3-\delta}$), 0.27 - 0.31 for electron-poor mixed conductors ($CaZr_{0.9}In_{0.1}O_{3-\delta}$, $SrFe_{0.0013}Ti_{0.9987}O_{3-\delta}$ perovskites), and 0.39 - 0.41 for electron-rich mixed conductors ($La_{0.8}Sr_{0.2}MnO_{3-\delta}$, $La_{0.6}Sr_{0.4}Fe_{0.8}Co_{0.2}O_{3-\delta}$ and $La_{0.3}Sr_{0.7}CoO_{3-\delta}$ perovskites) [3,4,13]. This assumes that different mechanisms are operative for electron-rich or electron-poor materials. The work reported by De Souza et al. also suggests a single theoretical expression of the pO_2 dependence of k* for all materials in agreement with experimental data, as determined by equation 17:

$$n = \frac{\partial \ln k^*}{\partial \ln pO_2} = A\left(\frac{\partial \ln C_h}{\partial \ln pO_2} + \frac{\partial \ln C_e}{\partial \ln pO_2}\right) - \frac{1}{2}\frac{\partial \ln C_v}{\partial \ln pO_2} + \frac{1}{4} \qquad \text{equation 17}$$

where c_h, c_e and c_v correspond to hole, electron defect, and oxygen vacancy concentrations, respectively. A is a pre-exponential value depending on each composition. The m value is mainly linked to the evolution with pO_2 of the ionic defect concentration because the electro-neutrality, in the peculiar case of electronic–rich mixed conductors, (c_h or c_e >> c_v) involves the following: $\frac{\partial \ln C_h}{\partial \ln pO_2} + \frac{\partial \ln C_e}{\partial \ln pO_2}$. Then, equation 17 becomes the following:

$$n = \frac{\partial \ln k^*}{\partial \ln pO_2} = -\frac{1}{2}\frac{\partial \ln C_v}{\partial \ln pO_2} + \frac{1}{4} \qquad \text{equation 18}$$

In the case of an interstitial oxygen conductor such as $La_2NiO_{4+\delta}$ nickelate, equation 18 becomes

$$n = \frac{\partial \ln k^*}{\partial \ln pO_2} = \frac{1}{2}\frac{\partial \ln C_i}{\partial \ln pO_2} + \frac{1}{4} \qquad \text{equation 19}$$

where c_i is the interstitial oxygen concentration.

However, equation 19 can be applied only if the system is a chemical equilibrium. For the isotopic exchange depth profile method, the system is at the chemical equilibrium. Unfortunately, for oxygen semi-permeation, the system is far from an equilibrium state, and the main assumptions of this model are not true.

Figure 5 shows the evolution of c_v for $La_{0.6}Sr_{0.4}Fe_{0.6}Ga_{0.4}O_{3-\delta}$ perovskite and c_i for $La_2NiO_{4+\delta}$ nickelate in relation to the oxygen partial pressure of the surrounding atmosphere. The measurements of C_v and C_i are obtained from thermal-gravimetric analysis at high temperature and atmosphere and lattice parameters determined by X-rays diffraction at high temperature.

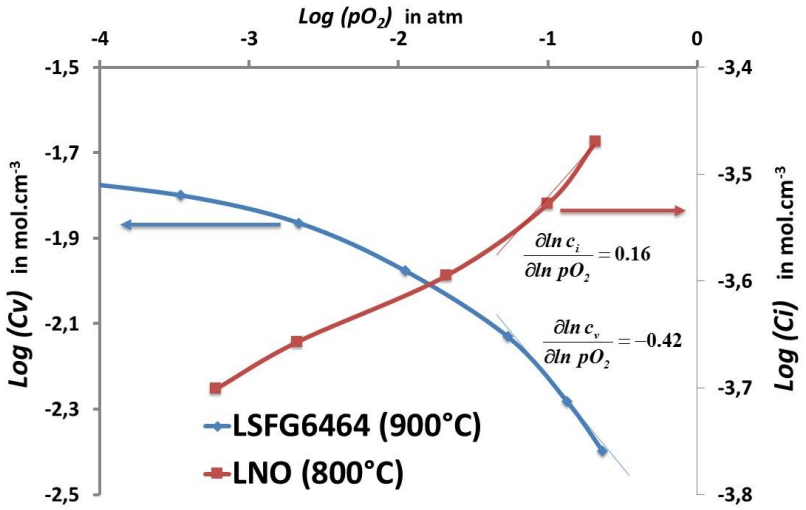

Figure 5: Determination of $\frac{\partial \ln C_V}{\partial \ln pO_2}$ or $\frac{\partial \ln C_i}{\partial \ln pO_2}$ values from the evolution of Log c_v or Log c_i vs. Log pO_2 for $La_{0.6}Sr_{0.4}Fe_{0.6}Ga_{0.4}O_{3-\delta}$ (LSFG6464) and for $La_2NiO_{4+\delta}$ nickelate (LNO) using thermo-gravimetric measurements at 900°C and 800°C, respectively [14,15].

The value of n from 210 mbar to 50 mbar is estimated at 0.46 for $La_{0.6}Sr_{0.4}Fe_{0.6}Ga_{0.4}O_{3-\delta}$ perovskite (LSFG6464) and 0.33 for $La_2NiO_{4+\delta}$ nickelate (LNO) (from equation 18 and 19, where n = 0.42/2 + ¼ and n = 0.16/2 + ¼, respectively), which is in good agreement with usual values reported in the literature for electronic-rich mixed conductor [13]. However, n significantly decreases with pO_2, for instance, n ~ 0.38 when pO_2 is lower than 10 mbar for $La_{0.6}Sr_{0.4}Fe_{0.6}Ga_{0.4}O_{3-\delta}$ perovskite.

The pO_2 dependence on D_O and k can be estimated from oxygen semi-permeation measurements with the large variation of the pO2 gradient between both membrane surfaces, as reported in Figure 3.

In Figure 6, the D_O coefficients for $La_{0.6}Sr_{0.4}Fe_{0.6}Ga_{0.4}O_{3-\delta}$ perovskite show low variation with pO_2 (close to 2-3 10^{-7} $cm^2.s^{-1}$). Conversely, D_O coefficients decrease significantly with for $La_2NiO_{4+\delta}$, from 2-3 10-7 to 2 10-8 $cm^2.s^{-1}$ when pO_2 decreases from 0.1 to 0.001. This trend is expected because the interstitial oxygen concentration in $La_2NiO_{4+\delta}$ decreases with pO_2. The decrease of interstitial oxygen concentration leads to the decrease of oxygen diffusion in $La_2NiO_{4+\delta}$ with pO_2.

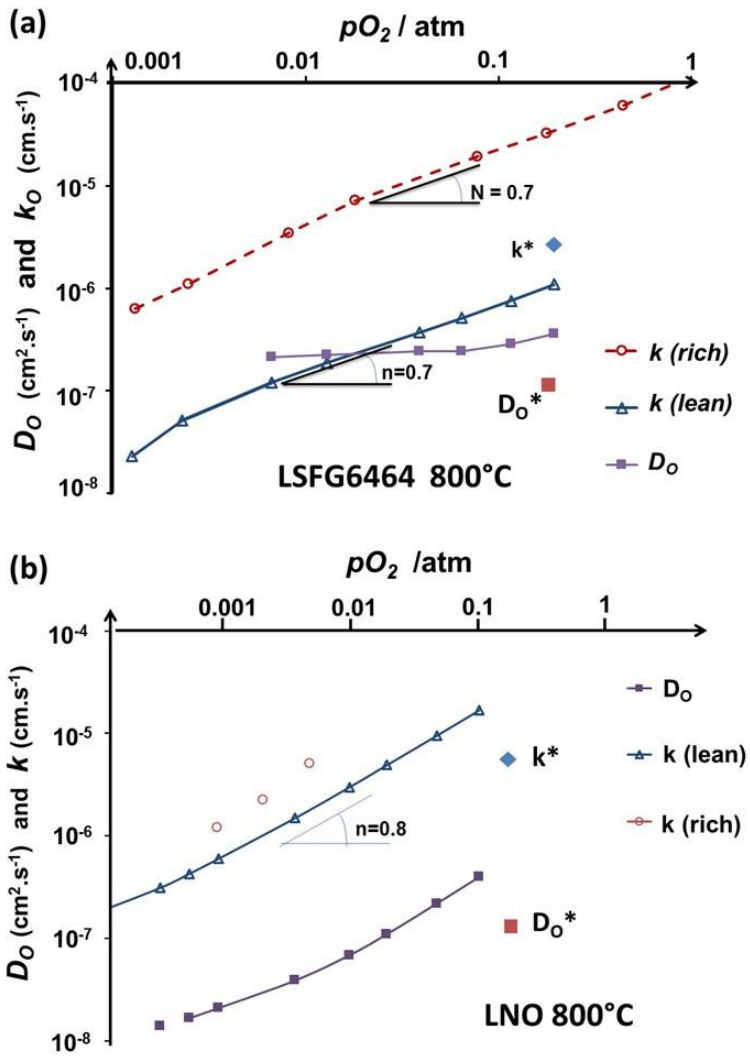

Figure 6: pO_2 dependence on D* and k* at 800°C for a) $La_{0.6}Sr_{0.4}Fe_{0.6}Ga_{0.4}O_{3-\delta}$ and b) $La_2NiO_{4+\delta}$.

In the opposite case, the oxygen vacancy concentration in $La_{0.6}Sr_{0.4}Fe_{0.6}Ga_{0.4}O_{3-\delta}$ perovskite increases with pO_2. The apparent low variation of the D_O coefficients in $La_{0.6}Sr_{0.4}Fe_{0.6}Ga_{0.4}O_{3-\delta}$ perovskite with pO_2 on Figure 5a is likely linked to two antagonist effects on oxygen bulk diffusion. The first one is linked to the increase of oxygen vacancy concentration with the pO_2 and the second one is linked to the decrease of mobility of oxygen vacancies with the increase of oxygen vacancy concentration in the perovskite structure. The impact of both effects leads to a low variation of Do with pO_2 in $La_{0.6}Sr_{0.4}Fe_{0.6}Ga_{0.4}O_{3-\delta}$ perovskite.

The n coefficient in the power law expressed previously in equation 16 can be estimated as 0.7 for $La_{0.6}Sr_{0.4}Fe_{0.6}Ga_{0.4}O_{3-\delta}$ and 0.8 for $La_2NiO_{4+\delta}$ membranes from the data reported in figure 5.

The exponent values designed by n, as reported in equations, 16, 18 and 19, can be evaluated from the slope of the curve reported in Figure 5. Note that n is close to 0.7 for $La_{0.6}Sr_{0.4}Fe_{0.6}Ga_{0.4}O_{3-\delta}$ perovskite and 0.8 for $La_2NiO_{4+\delta}$ nickelate. These values are significantly higher than those evaluated from the thermal gravimetry analysis and the usual values expected in the literature [3,4,13]. This apparent discrepancy could be linked to the starting hypothesis suggested in the model reported by De Souza et al., which assumes that the system is at equilibrium, while the oxygen semi-permeation measurements correspond to a system far from equilibrium [16,17].

The values obtained with both methods are similar for high pO_2 (=0.21), but the oxygen permeation measurements lead to an overestimation of the coefficients D and k, as reported in a recent study [14]. This apparent discrepancy suggests that the formalism applied for oxygen permeation must be considered in the case of a no equilibrium system. Another assumption is that one of the methods could be impacted by a systematic experimental error when pO_2 decreases, as previously reported in this work.

Furthermore, k decreases with pO_2 for both materials in Figure 6. This variation of k is likely linked to a large variation of oxygen concentration in both materials and the mismatch with ideal values, as suggested in Butler Volmer formalism. Although k^{rich} values are close to the k^{lean} values for the $La_2NiO_{4+\delta}$ membrane, a significant discrepancy is noted between k^{rich} and k^{lean} coefficients obtained with a $La_{0.6}Sr_{0.4}Fe_{0.6}Ga_{0.4}O_{3-\delta}$ perovskite membrane. Indeed, the oxygen semi-permeation measurements operate far from equilibrium at the interface solid/gas, particularly for the LSFG6464 membrane. This configuration allows the kinetics of oxygen adsorption or incorporation reaction at oxygen rich surfaces (reaction 1) to be isolated and the oxygen desorption reaction at oxygen lean surfaces (reaction 2).

$$\frac{1}{2}O_2 + V_O^{\bullet\bullet} \xrightarrow{k^{rich}} O_O^X + 2h^{\bullet} \qquad \text{reaction 1}$$

$$O_O^X + 2h^{\bullet} \xrightarrow{k^{lean}} \frac{1}{2}O_2 + V_O^{\bullet\bullet} \qquad \text{reaction 2}$$

In other works, k^{rich} and k^{lean} are associated with the surface exchange coefficient of incorporation and desorption, respectively.

Figure 7 shows the evolution of the oxygen flux in relation to the gradient of oxygen chemical potential through the membrane surface. Basically, these data provide new evidence that the linear relation is not adapted to describe the oxygen surface exchanges at the membrane surface. The values of the exponential factor (n) are estimated in this work as 2 for LSFG6464 and 8 for LNO membranes if the following relationship is assumed and the gradient of oxygen chemical potential is large:

$$J_{O_2} = A \exp\left(\frac{m}{RT}\Delta\mu_{O_2}^{surf}\right) \qquad \text{equation 20}$$

where m>0, and A is a constant.

Equations 10 and 16 suggest the following relationship between the oxygen fluxes, the oxygen partial pressure at the membrane surface and the gradient of the oxygen partial pressure through the membrane surface.

$$J_{O_2} = \frac{1}{2}\, k_0 \left(\frac{pO_2^{"}}{pO_2^{\circ}}\right)^n C_O \left(\exp\left(\frac{(1-\beta)}{2RT}\Delta\mu_{O_2}^{surf}\right) - \exp\left(\frac{-\beta}{2RT}\Delta\mu_{O_2}^{surf}\right)\right) \qquad \text{equation 21}$$

$pO_2^{"}$ is the oxygen partial pressure at the lean side. pO_2° is the reference oxygen partial pressure, usually pO_2° = 0.21 atm.

We can simplify equation 21, because we assumed that $J_{O_2} = B\, pO_2^{"}$ at the oxygen lean surface (see annex 2).

$$J_{O_2} = A \left(\exp\left(\frac{(1-\beta)}{2RT}\Delta\mu_{O_2}^{surf}\right) - \exp\left(\frac{-\beta}{2RT}\Delta\mu_{O_2}^{surf}\right)\right)^{\frac{1}{1-n}} \qquad \text{equation 22}$$

If $\Delta\mu_{O_2}^{surf} \gg RT$, equation 25 can be simplified as follows:

$$J_{O_2} = A \exp\left(\frac{(1-\beta)}{2(1-n)RT}\Delta\mu_{O_2}^{surf}\right) \qquad \text{equation 23}$$

$$\text{Or } m = \frac{(1-\beta)}{2(1-n)} \qquad \text{equation 24}$$

The m value is estimated as 2 for $La_{0.6}Sr_{0.4}Fe_{0.6}Ga_{0.4}O_{3-\delta}$ from the data reported in figure 7. In the case of $La_2NiO_{4+\delta}$ membranes, the oxygen activity gradient is too low for a suitable estimation of m because $\Delta\mu_{O_2}^{surf} \approx RT$. Then, the value of β can estimated as -0.2 for $La_{0.6}Sr_{0.4}Fe_{0.6}Ga_{0.4}O_{3-\delta}$. These values are inconsistent with values of β typically estimated in the literature between 0 and 1 [9,10].

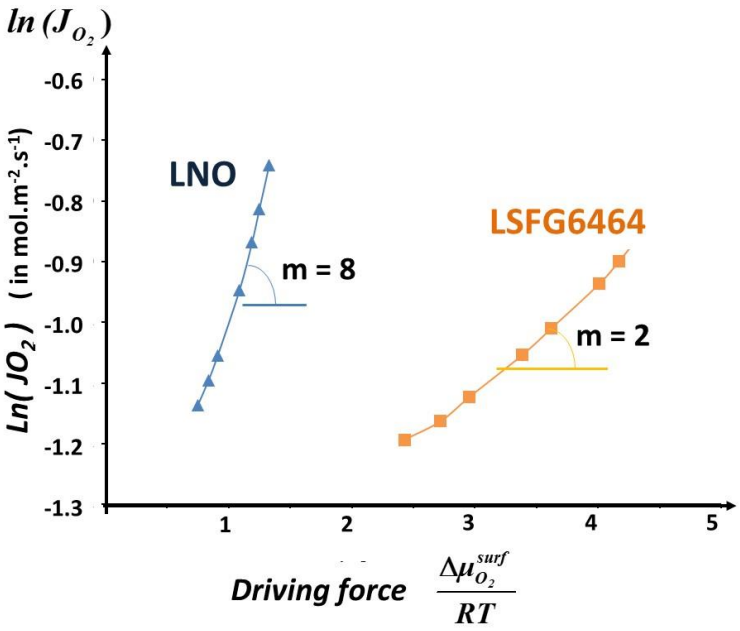

Figure 7: Determination of m from experimental data for the oxygen flux in relation to the oxygen chemical gradient potential at the surface of $La_{0.6}Sr_{0.4}Fe_{0.6}Ga_{0.4}O_{3-\delta}$ (LSFG6464) perovskite and $La_2NiO_{4+\delta}$ nickelate (LNO) membranes.

For a low oxygen chemical potential gradient, it is suggested that the actual accuracy of the semi-permeation setup is too low to observe the linear relationship for the low oxygen potential gradient at the membrane surface, as expected in equation 11.

For the large oxygen chemical potential gradient, the dependence of k on pO_2 could govern the evolution of oxygen flux with the oxygen chemical potential gradient.

However, figure 8b shows that the experimental curves can be reproduced for high values of n (with n=0.7) if the impact of the oxygen activity variation during oxygen measurements is considered, as expressed in equation 21. This confirms that the evolution of the oxygen flux with the oxygen chemical potential gradient in this work depends mainly on the following two terms: the dependence of k with pO_2 (linked by n exponent in equation 21 or 23) and the asymmetric potential linked to the polarization of the interface (linked by β coefficient). Finally, the data reported by semi-permeation measurements are consistent with the model reported by Bazant [10].

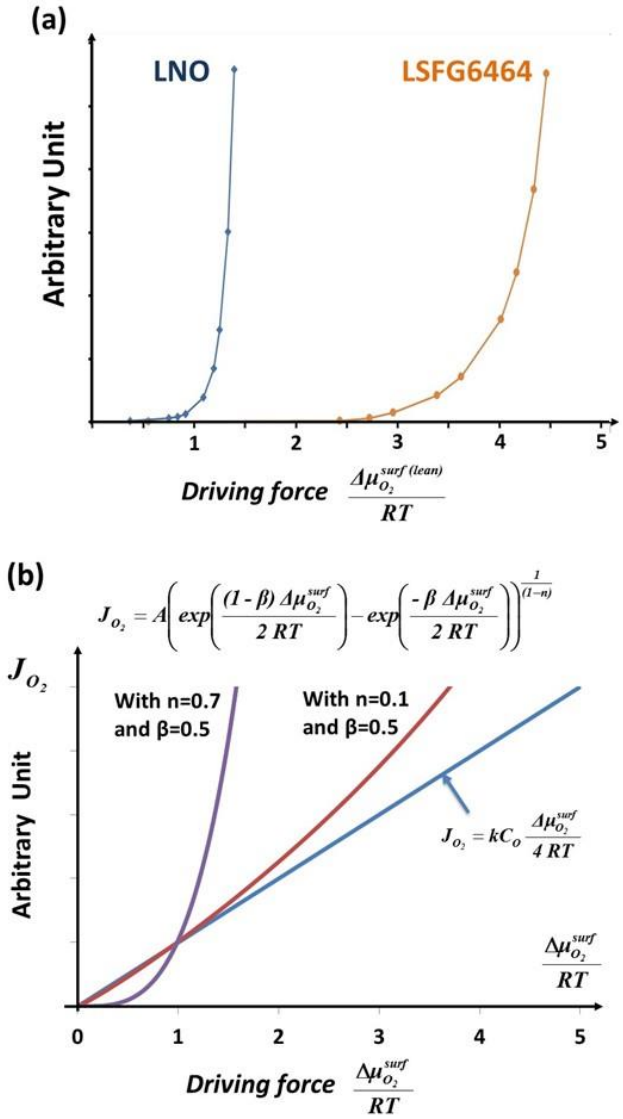

Figure 8: a) Experimental data for the oxygen flux in relation to the oxygen chemical gradient potential at the surface of $La_{0.6}Sr_{0.4}Fe_{0.6}Ga_{0.4}O_{3-\delta}$ (LSFG6464) perovskite and $La_2NiO_{4+\delta}$ nickelate (LNO) membranes. b) Theoretical curves expressed by equation 25, in relation to n and β parameters.

4. Conclusions

This study shows that the oxygen surface exchange coefficient of mixed conductors decreases significantly at low pO_2. It is assumed that the usual models regarding oxygen surface exchanges for oxygen semi-permeation measurements can lead to an important discrepancy for the values of k. The Butler-Volmer formalism, as reported in previous works, is adapted for the formalism of oxygen surface exchange kinetics on mixed conductors with a large driving force.

Furthermore, this work demonstrates that various conditions can be carefully checked with the IEDP method, in particular, low pO_2. This requires specific experimental conditions, such as a large volume chamber or a fixed concentration of ^{18}O in the chamber. Unfortunately, these conditions are not always considered in previous works. This study shows that the model reported by De Souza regarding the evolution of k* with pO2 could be not applied for systems far from equilibrium, such as oxygen transport membranes, or the solid oxide fuel cell. In this way, the oxygen semi-permeation method could be a judicious experimental method to establish the fundamental relationships between D_O, k, and pO_2.

References

[1] P.-M. Geffroy, A. Vivet, J. Fouletier, C. Steil, E. Blond, N. Richet, P. Del Gallo, T. Chartier, The impact of experimental factors on oxygen semi-permeation measurements, *J. The Electrochemical Society*, 160 (1), F1-F9 (2013).

[2] De Souza R.; Zehnpfenning J.; Martin M.; Maier J., *Solid State Ionics,* 2005, *176*, 1465-1471.

[3] R.H.E. Van Doorn, I.C. Fullarton, R.A. De Souza, J. Kilner, H.J.M. Bouwmeester, A.J. Burggraaf, Surface oxygen exchange of $La_{0.3}Sr_{0.7}CoO_{3-\delta}$, Solid State Ionics, 96 (1997) 1-7.

[4] R.A De Souza, J.A. Kilner, J.F. Walker, SIMS study of oxygen tracer diffusion and surface exchange in $La_{0.8}Sr_{0.2}MnO_{3+\delta}$, Mater. Lett. 43 (2000) 43

[5] A.V. Berenov, Oxygen tracer diffusion and surface exchange kinetics in La0.6Sr0.4O3, Solid State Ionics 181 (2010) 819-826.

[6] P.-M. Geffroy, A.Vivet, J. Fouletier, N. Richet, P. Del Gallo, T. Chartier, Influence of oxygen surface exchanges on oxygen semi-permeation through $La_{(1-x)}Sr_xFe_{(1-y)}Ga_yO_{3-\delta}$ dense membranes, *J. Electrochem. Soc.*, 158 (8) (2011) 1-9.

[7] C. Wagner, Equations for transport in solid oxides and sulfites of transition metal, Progress in Solid State Chemistry, Pergamon Press, 10, Part 1, 3-16, (1975).

[8] G.E. Murch, The haven ration in fast ionic conductors, Solid State Ionics 7 (1982) 177-198.

[9] S. B. Adler, X. Y. Chen, J. R. Wilson, Mechanisms and rate laws for oxygen exchange on mixed-conducting oxide surfaces, Journal of Catalysis, 245 (2007) 91-109.

[10] M.Z. Bazant, Theory of chemical kinetics and charge transfer based on nonequilibrium thermodynamics, Accounts of chemical research 46, 5 (2013), 1144-1160.

[11] S. Kim, Y.L. Yang, A. J. Jacobson, B. Abeles, Oxygen surface exchange in mixed ionic electronic conductor membranes, Solid Sate Ionics 121 (1999) 31-36.

[12] H.J.M Bouwmeester, Dense ceramic membranes for methane conversion, Catal. Today, 82 (2003) 141-150.

[13] R.A. De Souza, A universal empirical expression for the isotope surface exchange coefficients (k*) of acceptor-doped perovskite and fluorite oxides, Physical Chemistry Chemical Physics, 8 (2006) 890.

[14] P.-M. Geffroy, Y. Hu, A. Vivet, T. Chartier, G. Dezanneau, Determination of oxygen diffusion coefficients in $La_{1-x}Sr_xFe_{1-y}Ga_yO_{3-\delta}$ perovskites using oxygen semi-permeation and conductivity relaxation methods, *J. Electrochemical Society,* 161 (3), F153-F160 (2014).

[15] A. Flura, S. Dru, C. Nicollet, V. Vibhu, S. Fourcade, E. Lebraud, A. Rougier, J.-M. Bassat, J.-C. Grenier, Chemical and structural changes in $Ln_2NiO_{4+\delta}$ (Ln=La, Pr or Nd) lanthanide nickelates as a function of oxygen partial pressure at high temperature, Journal of Solid State Chemistry, 228 (2015) 189-198.

[16] J. Maier, On the correlation of macroscopic and microscopic rate constant in solid state chemistry, Solid State Ionics, 112 (1998) 197-228.

[17] M.H.R. Lankhort, H.J.M. Bouwmeester, H. Verweij, Thermodynamics and transport of ionic and electronic defects in crystalline oxides, J. Am. Ceram. Soc. 80, 9 (1997) 2175-2198.

Annex 1

at 800°C	*Vm (Å^3)*	δ_{air}	δ_{Ar}	*C_O (mol.cm^{-3}) at pO_2= 0.21 atm)*	*C_O (mol.cm^{-3}) at $pO_2 \approx 10^{-4}$ atm*
LNO	97.5 (= 390/4)	0.08	0.047	$6.95\ 10^{-2}$	$6.89\ 10^{-2}$
$LSFG_{6464}$	59.78	0.136	0.18	$7.96\ 10^{-2}$	$7.80\ 10^{-2}$

Table 2: Oxygen molar concentration (Co) under air and nitrogen for LSFG6464 perovskite and LNO nickelate at 800°C.

Annex 2

The oxygen semi-permeation fluxes can be calculated from the values of pO_2'' and Equation 25 when the oxygen flow ($J_{O_2} \times S$) through the membrane (in ml.s^{-1}) is significantly lower than the inlet argon flow in chamber 2, corresponding to 200 ml.s^{-1}. In general, the argon atmosphere is preferred for oxygen flux measurements to achieve higher sensitivity and accuracy for low variations in oxygen content.

$$J_{O_2} = \frac{D_{Ar}}{V_m}\left(\frac{pO_2'' - pO_{2\,(in)}}{S}\right) \qquad \text{equation 25}$$

J_{O_2}: oxygen flux through the membrane in mol.m^{-2}.s^{-1},
D_{Ar}: argon flow in l.s^{-1} (= 3.33 10^{-3} l.s^{-1}),
V_m: molar volume of argon in l.mol^{-1} (= 24 l.mol^{-1} at 20°C under 1 atm),
S: efficient membrane surface or membrane section (= 3.14 10^{-4} m^2),
pO_2'': oxygen partial pressure in the argon flux outlet (in atmosphere),
$pO_{2\,(in)}$: oxygen partial pressure in the argon flux inlet (≈10^{-6} atm).

As $pO_2'' >> pO_{2\,(in)}$, we can simplify equation 25 as follows:

$$J_{O_2} = \frac{D_{Ar}}{V_m}\left(\frac{pO_2''}{S}\right) => B\ pO_2'' \text{ with B as a constant.} \qquad \text{Equation 25}$$

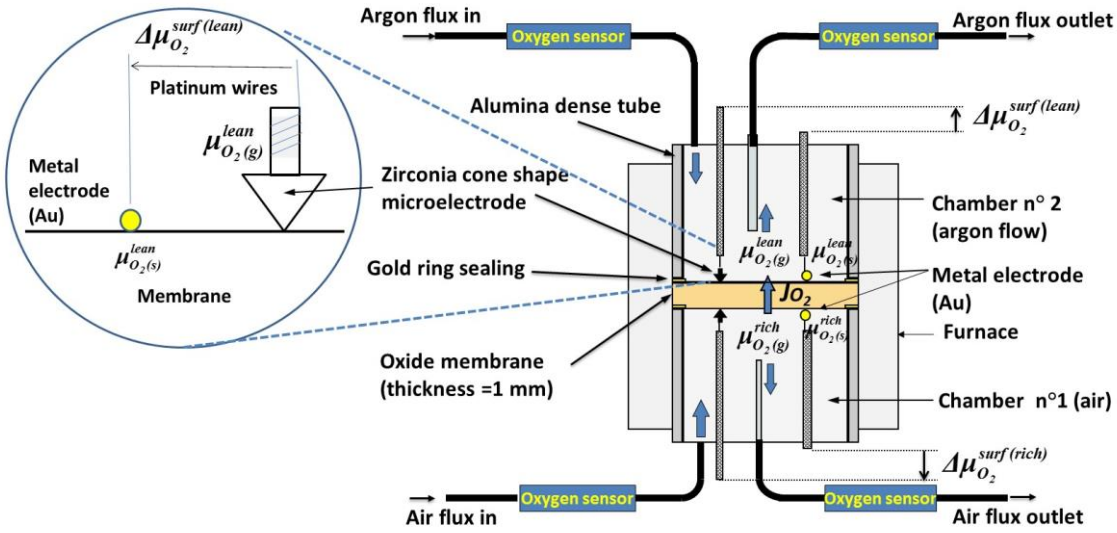

Figure 9: Setup for oxygen semi-permeation measurements with the zirconia cone shape and gold microelectrodes for the measures of oxygen activity at the membrane surfaces [1].